

*Досліджено основні фактори формування пористості пресованих виробів на основі губчастого титану. Виділено три види пор – кластерні (на місці частинок), міжкластерні та власні пори матеріалу. Розроблено кластерні моделі упаковки частинок на стадіях пресування (від насипної щільності, або формування тимчасових структур до формування стабільних структур). Число граней кластерів в моделях залежить від координаційного числа  $\lambda$ , що означає тетраедричні ( $\lambda=4$ ) кластери на початковій стадії та кубооктаедричні ( $\lambda=12$ ) на пізніх. На основі правила Гаусса для упаковки куль визначено, що найбільш правильною формою кластерів для пізніх стадій пресування є кубооктаедр, так як пори між кулями при максимальній щільній упаковці з координаційним числом 12 мають форму близьку до кубооктаедрів та октаедрів, але з увігнутими гранями. На основі різниці між об'ємами куль, за які прийнято частинки та кластерів в моделі, спираючись на розраховані об'єми міжкластерних октаедрів та кубооктаедрів було обчислено об'єм пор, які мають форму штейнерівського октаедра чи кубооктаедра. При розрахунку міцності зчеплення між частинками власна пористість губчастого титану визначається через припущення, що частинка порошку є конгломератом, який формується з порожнистих куль правильної форми на стадії відновлення титану магнійтермічним методом. Відповідно, в формулі розрахунку міцності зчеплення сила, що діє на частинку складатиметься з різниці сил пружної деформації та руйнування порожнистих куль, що містяться в деформованому об'ємі. Розроблені моделі підтверджено результатами практичних досліджень. Реальні вимірювання демонструють середнє експоненціальне відношення пористості до тиску пресування, що дозволяє розрахувати максимальну міжкластерну пористість при граничному ущільненні в 66 % та коефіцієнт стиснення досліджуваного матеріалу в 0,15*

*Ключові слова: композити, порошкова металургія, губчастий титан, упаковка часток, пресування, типи пор*

UDC 669.295-026.564.4-135:62-4-026.564.3  
DOI: 10.15587/1729-4061.2020.206715

# CLUSTER MODEL OF THE POROSITY OF SPONGY TITANIUM BRIQUETTES AT THE STAGE OF PRESSING

**L. Klymenko**

Doctor of Technical Sciences, Professor, Rector\*  
E-mail: rector@chmnu.edu.ua

**V. Andreev**

PhD, Associate Professor\*  
E-mail: avi@chmnu.edu.ua

**O. Sluchak**

Senior Researcher  
Scientific Research Part\*\*\*  
E-mail: slu4ok@gmail.com

**O. Pryshchepov**

PhD, Associate Professor\*\*  
E-mail: priof@ukr.net

**O. Shchesiuk**

PhD, Associate Professor\*\*  
E-mail: taifun.kv@gmail.com

\*Department of Ecology and Environmental Management\*\*

\*\*Department of Automation and Computer-Integrated Technologies

\*\*\*Petro Mohyla Black Sea National University  
68 Desantnykiv str., 10,  
Mykolayiv, Ukraine, 54003

Received date 27.04.2020

Accepted date 10.06.2020

Published date 30.06.2020

Copyright © 2020, L. Klymenko, V. Andreev, O. Sluchak, O. Pryshchepov, O. Shchesiuk

This is an open access article under the CC BY license

(<http://creativecommons.org/licenses/by/4.0>)

## 1. Introduction

Spongy titanium is a highly porous material, obtained by reducing titanium chloride by magnesium at titanium-magnesium mills by the Kroll method. After separation, it is used as raw material to obtain powders of titanium nitrides, carbides, and borides, or smelting metallic titanium.

Active titanium production [1] as a high-capillary material, indicates the significant value of such characteristics as porosity for material science, medical industry, electric welding, atomic energy, etc.

There is no single porosity classification. While according to the typology, porosity can be divided into open, closed, and isolated, porous bodies are often divided into corpuscular and spongy [2]. In corpuscular porosity, the body base is particles surrounded by voids in the form of pores, and in spongy po-

rosity, the pores themselves form the body structure, while the material surrounds them by a kind of frame.

The use of a corpuscular-spongy classification of porous bodies is caused by the fact that it perfectly describes the resulting cluster model. This approach makes it possible to describe most fully the properties of porosity of pressed spongy titanium briquettes.

The relevance of this study is related to the need to develop theoretical substantiation of the processes of the formation of porosity of products based on spongy titanium at the pressing stage. This is supplemented by practical proof of the developed concepts for their further application in the development of composite materials with volume variable thermo-physical properties. It is implemented by controlling porosity, and subsequently by the methods of its surface or volume regulation.

Thus, the exact knowledge of the porosity nature will make it possible to predict the thermophysical properties of obtained materials due to the combination of conduction (the Lobb formula), convection (Navier-Stocks equation, and Benar-Marangoni effect) and thermal radiation (the Kirchhoff law). This will allow obtaining composite materials with given thermo-physical properties for foundry production. In addition, highly capillary materials with the known threshold structure for medicine and filters are promising as well.

---

## 2. Literature review and problem statement

---

The development of powder metallurgy as an industry within materials science is convergent in nature and, therefore, affects a significant number of other industries.

Most of the publications, associated with spongy titanium, do not imply its direct application in composite materials. Often it is the raw material for obtaining titanium hydrides and nitrides or a semi-finished product for melting into metal ingots. The essential part of the publications, related to titanium powder metallurgy, has medical orientation [3]. In addition, it is used in obtaining consumable electrodes for welding, forming the cases of power units of nuclear power plants, and as passive cooling in the systems of automation of centrifugal casting of cylindrical parts. In recent years, the number of publications related to the use of titanium powders in the production of composite materials has decreased almost by two times. Until 2015, there were over 10 publications on titanium powder metallurgy per year.

Paper [4] contains the results of the studies of the interaction between the particles in powder composites on the interphase boundary. The possibilities of combination by the pressure of ceramics with metals, metals with metals and ceramics with ceramics through a plastic metal gasket were shown. The mechanism of the interaction of metals with oxide films at plastic deformation was revealed. One of the given examples is the application of titanium powders, nitrides, and titanium carbides in composites. However, as a part of the research into the interaction on the inter-phase boundary, the behavior of pressing in the volume was not revealed.

Article [5] revealed the specific features of density distribution in radial pressing. However, the data obtained in the process of research are averaged and do not enable characterizing the peculiarities of the zonal density distribution, depending on loading.

A variant of solving this problem can be the use of mechanical fatigue and plastic flow as a determining factor of the transformation of the structure of pressing. Such a generalized approach was applied in study [6]. But the issues of interaction of rough surfaces with a random structure, in particular in the case of spongy titanium, remain unresolved. The reason for this can be objective factors related to the complexity of modeling the structure of such a surface and subjective factor, related to the authors' specialization.

A variant of the solution to this problem can be considered the specialized research into pressing based on spongy titanium. This approach is applied in study [7]. However, the behavior of a separate particle of such a powder when interacting with the neighboring particles was not explored in this case. In addition, porosity in their model is considered in the general form (a pore is equal to a sphere).

Paper [8] presented the multi-criteria approach using the perfect point method. The approach was based on earlier research by authors of [9], related to modeling the plastic flow of spongy titanium within one particle using the Drucker-Prager curve, which was approximated through Bernoulli lemniscate. The same approach is applied in article [10]. However, in this case, the stressed state of the material was taken into consideration, which makes the model more complete. However, both cases did not take into consideration such a decisive factor as powder particle arrangement in the pressing. In addition, the model of their packing, which was the basis for the calculations [9, 11], has a cubic lattice, which does not correspond to the actual structure of packing spherical particles in the densest pressing.

The issue of homogenization of spongy titanium was explored in paper [12]. The study was based on an earlier model [13], where a particle was seen in the flat cut in the form of a honeycomb, which allowed simulating the distribution of stresses in it under the elastic punch. However, although in a flat cut, the space filling with honeycombs displays the most compact packing, packing the particles in the volume of pressing was not taken into consideration.

The creation of a clustered model of packing particles in pressing will make it possible to predict more accurately the properties of the future material. Taking into consideration the features of the structure of spongy titanium as a conglomerate of hollow titanium spheres, as well as the coordinates of particles will create a clear idea of the structure of a pressed briquette. A clear idea of the structure will make it possible to describe more efficiently the stress distribution. The distribution of stresses, in turn, will provide an opportunity to predict an elastic post-effect in pressing out, gripping strength, and sintering temperature to correct these data.

Accordingly [14], the porosity of samples based on spongy titanium of the TG-TV brand can be controlled by pressing pressure and the methods of surface and volumetric closure of porosity, providing the necessary thermal and physical properties for their application in casting molds. In this case, such composite covers automate the process of crystallization of the cast due to passive regulation of heat removal rate.

Despite the practical significance of such results, the obtained data require a theoretical base, because deviations in porosity at the local level can be quite significant.

The relevance of studying the modeling of the processes of the formation of porosity of spongy titanium products is proved by their wide application as medical implants, consumable electrodes, and filters. In the long term, it is proposed to obtain materials for casting molds, as systems of passive cooling the casts in the process of automation of centrifugal casting. The methods for obtaining protective elements for military-civilian purposes are also being developed.

Therefore, there are some grounds to believe that control of porosity at the early stages of pressing will make it possible to comprehensively influence the properties of materials received. This approach in synergy with the porosity closing methods will enable obtaining materials with a wide range of properties from the same components.

---

## 3. The aim and the objectives of the study

---

The purpose of the conducted research is the development and experimental substantiation of the cluster model of

pressed products of spongy titanium at the stage of pressing composite briquettes.

To achieve the set aim, the following tasks were solved:

- focusing on coordinate numbers at each stage, to develop a cluster model of forming and arranging cluster and intercluster pores in a mold relative to the weight centers of particles;
- to calculate the coordinates of the contact points of a particle with neighboring particles relative to the geometric center of its cluster, which under real conditions will be in the center of particle’s weight;
- based on the hypothesis that spongy titanium is a conglomerate of hollow spheres formed during its obtaining, to draw up the formula of load distribution at isostatic pressing;
- to conduct measurements of actual porosity and density of pressing and to determine the patterns of their dependence on pressing loading.

**4. Materials and methods to study the porous workpieces of composite materials with a differentiated volumetric structure based on titanium sponge until the sintering stage**

**4.1. Studied materials and equipment used in the experiment**

The study was carried out using the equipment to press the experimental samples in the form of the hardened steel mold, ground to Ra3,2 (Fig. 1); re-equipped discontinuous machine of the R-10 model; drying chamber SC-20.

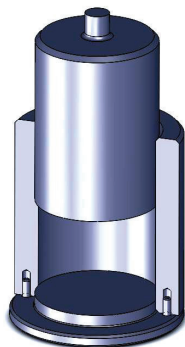


Fig. 1. Press mold for obtaining experimental samples of porous materials with different porosity

The shape and dimensions of the experimental samples were determined according to regulated parameters for testing the strength of the material on the press equipment (for the P-10 rupture machine) and the technological capacities of a vacuum furnace for subsequent sintering.

The samples were analyzed through the metal microscope Nikon Z100 (office “CIS TokyoBoekiLtd”, Kyiv). The grain size was determined by the assessment according to the standard scales E19 ASTM using the Jeffries method and made up: the specific surface of a grain  $\Delta=56 \text{ mm}^2/\text{mm}^3$ ; The number of grains per  $1 \text{ mm}^2$  ( $n$ )=43.

Actual open porosity was measured using the microphotograph gate method.

The study of the chemical composition of pressing was conducted on the plant of phase-structural analysis DRON-3.

The experimental samples of composite materials were prepared by mixing the crushed titanium sponge TG-Tv (fraction–3.3+1.3 mm) in the form of briquettes with a porosity of 30–65 %.

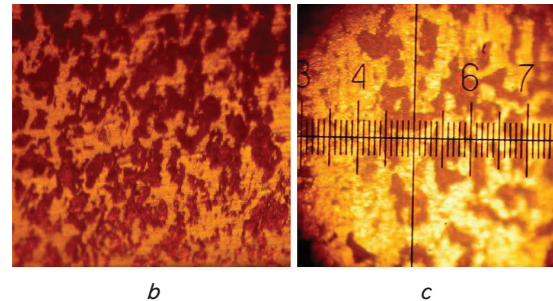
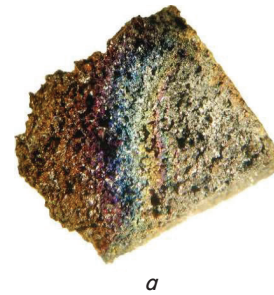


Fig. 2. A sample through a metal graphic microscope Nikon Z100 (the rep office of CIS Tokyo Boeki Ltd, Kyiv) – in polarized light: *a* – test sample, *b* – polarized light micrograph, *c* – measuring scale E19 ASTM

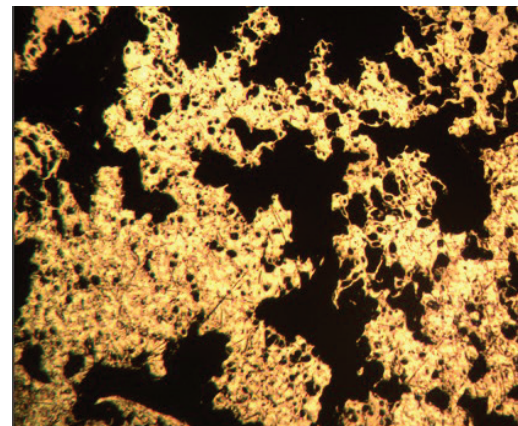


Fig 3. Microphotograph of a pressed spongy titanium briquette

**4.2. Research methodology and main hypotheses**

The bulk density of spongy titanium was measured experimentally by multiple repetitions and averaging and was determined from formula (1):

$$\rho_{bulk} = \frac{m_{ST}}{V_{ST}}, \tag{1}$$

where  $\rho_{bulk}$  is the bulk density,  $m_{ST}$  is the weight of spongy titanium without fillers,  $V_{ST}$  is the powder volume.

In this case, the parameters of one particle (2) to (5):

$$V_{particle} = \frac{4}{3}\pi R^3 = 1.15034650999 \text{ mm}^3, \tag{2}$$

$$S_{sphere} = 4\pi R^2 \approx 8.16814089933 \text{ mm}^2, \tag{3}$$

$\rho_{c.m.} = 4.54 \cdot 10^{-3} \text{ g/mm}^3$ , by the result of measuring at an analytical balance. Mass



$$m_{particle} = \rho_{c.m.} \cdot V_{particle} \cdot (1 - P_{own}) = 6.81157315535 \cdot 10^{-3} \cdot (1 - P_{own}) \text{ g,}$$

in one particle (4).

For further calculations, it is necessary to compute the natural porosity of particles (5). The calculations below give the expected porosity in

$$P_{own} = \theta_{\Sigma ST} = 1 - \frac{\rho_{\Sigma n_v}}{\rho_{Ti}} = 0.67055587873, \quad (5)$$

accordingly,  $m_{particle} = 0.00224403273$ .

The porosity of the finished material was determined by finding the gate by the microphotography method.

Based on the conducted observations, a series of hypotheses were put forward:

1. The arrangement of particles and pores in the structure of the material produced by powder metallurgy methods is determined by three factors: coordination number  $\lambda$ , proper porosity of the powder, dimensions, and nature of particles' surface. It makes it possible to classify the porosity type not only as open, closed, and isolated, but also as proper, intersperse (between particles) and cluster (in the place of particles at packing defects).

2. Since particles are accepted as a conventional sphere, their most compact arrangement in a pressing product can correspond to one type of packing: face-centered cubical (FCC), hexagonal close packed (HCP), or Barlow random packing. This makes it possible to identify inflect cuboctahedrons and octahedrons as the most likely types of pores, and a hexagon and a triangle as the most likely cross-sections of these pores.

3. Spongy titanium consists of a conglomerate of hollow spheres that form its porosity. These spheres are formed at obtaining spongy titanium in the processes of its magnesium thermal formation and have different dimensions, forming a typical Apollonian packing within one particle of powder accepted as a sphere. Based on the statistical calculation, it is possible to determine the strength of compression of such particles when pressing based on the sum of force required to destroy the spheres and the force required to deform the metal they are formed of.

## 5. Results of the simulation of cluster porosity of spongy titanium briquettes in the framework of the corpuscular-spongy classification of porous bodies

5.1. A cluster model of the spatial structure of briquettes from compressed spongy titanium at the compaction stage

The stage of mechanical formation of composite materials [15] by pressing can be divided into 4 stages:

- 1) formation of unstable spatial structures;
- 2) formation of stable structures;
- 3) the stage of micro deformation of the volume of powder particles;
- 4) the stage of volume flow.

The first stage is the formation of unstable spatial structures that characterizes the conglomerate of composite elements in the state of free bulking and exhibits an unstable structure, dependent on granulometric composition, bulk density, fluidity, and specific surface of components. One of the main indicators characterizing the spatial structure of the elements of material at this stage is coordination number  $\lambda$ , which determines the

number of contacts between the adjacent particles and at the first stage should not exceed number 4.

The second stage of compaction involves the formation of the densest packing of particles that are tangent to each other.

In the volumetric representation at  $\lambda=12$ , dense packing is represented by layer arrangement of spheres in space. Carl Friedrich Gauss proved that the maximum density (6) that can be achieved by packing such spheres within a regular lattice.

$$\eta_h = \frac{\pi}{3\sqrt{2}} \approx 0.74048. \quad (6)$$

Packing such layers in the actual mold is presented by aperiodic in the direction of packing the layers of the non-periodic arrangement of Lagrange planes. In combinatorial geometry, such packing is called "Barlow packing". However, since there are a lot of variants of arrangement at this packing, the spatial placement of particles can be represented in the form of models for three layers.

There are three main types of such packing – face-centered cubic packing (FCC), hexagonal close packing (HCP), and irregular Barlow packing [15] (Fig. 4–6).

According to Kepler's hypothesis, proved in 1998 [16] with the help of program choice of variants, the FCC packing and HCP lattices are the most compact among periodic packings.

Both packing types have two layers, arranged so that a sphere in the second one should be located above the gaps in the first one. If the spheres of the third layer are located in the same plane as the spheres of the first layer (above them), such packing will be called hexagonal close-packed (HCP). If they are located above the gaps in the first layer, it will be called a face-centered cubic (FCC) [18].

Accordingly, each particle can be represented in the form of a cluster – polyhedron that will be a cluster pore in the concave form at the appearance of a defect in material formation (Fig. 5). The gaps between them will represent the figures, the concave (Steiner [19]) version of which will be a real form of intercluster pores (Fig. 7).

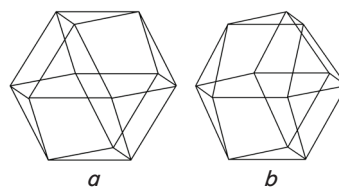


Fig. 4. FCC and HCP lattices for packing equal spheres:  
a – cuboctahedral FCC packing,  
b – inverse cuboctahedral HCP packing

That is why a simple powder composite formed by particles of the sphere-close shape is a typical corpuscular porous body that makes it possible to express clearly the position of particles and pores in a geometrical model.

### 5.2. Calculation of the coordinates of contact points of a particle with neighboring particles relative to the geometric center of a cluster

Since the main cuboctahedron symmetry plane is a hexagon, the radius of a sphere-particle, circumscribed around a cuboctahedron, will be equal to the radius circumscribed around the hexagon of a circle, which is equal to the length of the edge of the hexagon, and, accordingly, of the cuboctahedron  $R=a$ .

The coordinates of the vertices, which are the points of contact with the neighboring particles, assign the coordinates of two opposing triangles and a hexagonal cross-section. If the center of the circumscribed circle is the center of coordinates, the coordinates of the contact points can be represented as a table (Table 1).

Table 1

Coordinates of contact points in the FCC packing

Point	$x$ FCC(HCP)	$y$ FCC(HCP)	$z$ FCC(HCP)
1	$x_0 - \frac{\sqrt{3}}{6}a; \left(x_0 - \frac{\sqrt{3}}{6}a\right)$	$y_0 + \sqrt{\frac{2}{3}a^2}; \left(y_0 + \sqrt{\frac{2}{3}a^2}\right)$	$z_0 - \frac{a}{2}; \left(z_0 - \frac{a}{2}\right)$
2	$x_0 - \frac{\sqrt{3}}{6}a; \left(x_0 - \frac{\sqrt{3}}{6}a\right)$	$y_0 + \sqrt{\frac{2}{3}a^2}; \left(y_0 + \sqrt{\frac{2}{3}a^2}\right)$	$z_0 + \frac{a}{2}; \left(z_0 + \frac{a}{2}\right)$
3	$x_0 + \frac{\sqrt{3}}{3}a; \left(x_0 + \frac{\sqrt{3}}{3}a\right)$	$y_0 + \sqrt{\frac{2}{3}a^2}; \left(y_0 + \sqrt{\frac{2}{3}a^2}\right)$	$z_0; (z_0)$
4	$x_0 - \frac{\sqrt{3}}{2}a; \left(x_0 - \frac{\sqrt{3}}{2}a\right)$	$y_0; (y_0)$	$z_0 - \frac{a}{2}; \left(z_0 - \frac{a}{2}\right)$
5	$x_0 - \frac{\sqrt{3}}{2}a; \left(x_0 - \frac{\sqrt{3}}{2}a\right)$	$y_0; (y_0)$	$z_0 + \frac{a}{2}; \left(z_0 + \frac{a}{2}\right)$
6	$x_0; (x_0)$	$y_0; (y_0)$	$z_0 - a; (z_0 - a)$
7	$x_0; (x_0)$	$y_0; (y_0)$	$z_0 + a; (z_0 + a)$
8	$x_0 + \frac{\sqrt{3}}{2}a; \left(x_0 + \frac{\sqrt{3}}{2}a\right)$	$y_0; (y_0)$	$z_0 - \frac{a}{2}; \left(z_0 - \frac{a}{2}\right)$
9	$x_0 + \frac{\sqrt{3}}{2}a; \left(x_0 + \frac{\sqrt{3}}{2}a\right)$	$y_0; (y_0)$	$z_0 + \frac{a}{2}; \left(z_0 + \frac{a}{2}\right)$
10	$x_0 - \frac{\sqrt{3}}{3}a; \left(x_0 - \frac{\sqrt{3}}{6}a\right)$	$y_0 - \sqrt{\frac{2}{3}a^2}; \left(y_0 - \sqrt{\frac{2}{3}a^2}\right)$	$z_0; \left(z_0 - \frac{a}{2}\right)$
11	$x_0 + \frac{\sqrt{3}}{6}a; \left(x_0 - \frac{\sqrt{3}}{6}a\right)$	$y_0 - \sqrt{\frac{2}{3}a^2}; \left(y_0 - \sqrt{\frac{2}{3}a^2}\right)$	$z_0 - \frac{a}{2}; \left(z_0 + \frac{a}{2}\right)$
12	$x_0 + \frac{\sqrt{3}}{6}a; \left(x_0 + \frac{\sqrt{3}}{3}a\right)$	$y_0 - \sqrt{\frac{2}{3}a^2}; \left(y_0 - \sqrt{\frac{2}{3}a^2}\right)$	$z_0 + \frac{a}{2}; (z_0)$

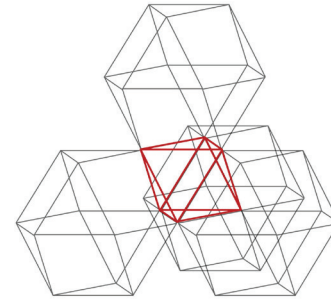


Fig. 5. Octahedral pore (FCC)

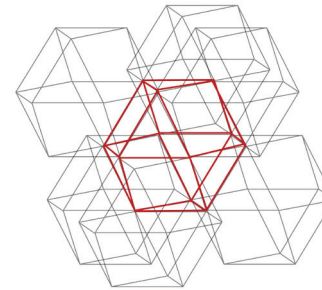


Fig. 6. Cuboctahedral pore (FCC)

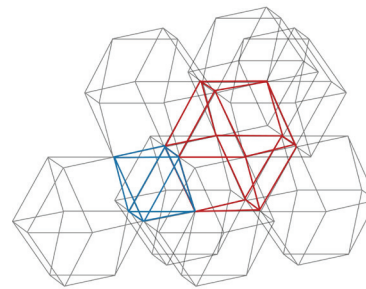


Fig. 7. Connection of an octahedral and cuboctahedral pores (HCP)

It is obvious that only  $z_0$  – the coordinate in three points – is different in two types of packing.

The volume of such a cluster formed around one particle can be calculated by summing up the volumes of thirteen cuboctahedrons (7), schematically representing a particle and a pore around them:

$$V = \frac{5a^3}{3}\sqrt{2}. \tag{7}$$

The shape of pores (Fig. 3–5) is represented by two types – 6 cuboctahedrons, similar to particles (by three in the upper and lower belt) and 8 octahedrons (by one at the top and at the bottom and by three in the upper and lower belt). Moreover, particles in FCC packing are arranged precisely over the cuboctahedron pores, which gives a pore with 8 faces, half of which are open transitions, connecting the specified pore with the neighboring one.

Accordingly, the total volume of a virtual cluster (8) will be slightly less than the volume of an actual cluster, but it can become the basis for its calculation:

$$V_{cluster} = \frac{95\sqrt{2}a^3}{3} + \frac{8}{3}\sqrt{2}a^3 = \frac{103\sqrt{2}a^3}{3}. \tag{8}$$

Thus, actual pores will represent polyhedrons, similar to those in the model, but with concave faces due to the curvature of spheres-particles. Accordingly, their actual volumes can be calculated by subtracting the parts, cut-off by the sphere, from the corresponding volume. To calculate the volume of the cut-off parts, it is necessary to subtract from the sphere segment, the base of which is the circle circumscribed around a face of the cluster cuboctahedron, the sections, cut off it when taking the face as a base. Such sections are the segments in the form of the quarters of the ellipsoid granule, the radii of which are equal for a triangular face (9) and (10):

$$R_1 = R_2 = r = \frac{\sqrt{3}}{6}a; \tag{9}$$

$$R_3 = \frac{a}{2}. \tag{10}$$

For a quadrangle, similar to (11) and (12)

$$R_1 = R_2 = \frac{2R_{descr} - a}{2} = \frac{(\sqrt{2}-1)a}{2}; \tag{11}$$

$$R_3 = \frac{a}{2}. \tag{12}$$

Accordingly, the volume of a granule is equal to the volume of an ellipsoid (13), which makes it possible to calculate the volumes of the sections cut off from the sphere segment in the form of the quarters of a granule as a determined total volume (14) for three triangular faces and total volume (15) for four quadrangular ones:

$$V_{face} = \frac{4}{3}\pi R_1 R_2 R_3; \quad (13)$$

$$V_{ato\,fragm.} = \frac{a^3}{288}\pi; \quad (14)$$

$$V_{ato\,fragm.} = \frac{12a^3 - 8a^3\sqrt{2}}{96}\pi. \quad (15)$$

Thus, at the volume of the sphere segment equal to the volume of the segment (16), on condition of equality to the radius of cuboctahedron to its side, the value of the radius, expressed through the length of the side and the height, is retained (17). Then one can state that for a square face, the ratio is retained in the form of square equation (18). Accordingly, there is a possibility to equate the square of the difference between the side and the height to half the side square (19). Therefore, one can determine the height from the length of the side (20):

$$V_{segm.} = \frac{\pi h}{6}(3r_{base}^2 + h^2); \quad (16)$$

$$r_{base} = \sqrt{2ah - h^2}; \quad (17)$$

$$a^2 - 2ah + h^2 = \frac{1}{2}a^2; \quad (18)$$

$$(a - h)^2 = \frac{1}{2}a^2; \quad (19)$$

$$a - \frac{a}{\sqrt{2}} = h. \quad (20)$$

Accordingly, the volume of the pore fragment, cut off by a particle on a quadrangular face, can be expressed through the length of a cluster side (21)

$$V_{quadr.\,fragm.} = \frac{\pi\left(a^3 - \frac{a^3}{\sqrt{2}}\right)}{6}\left(3 - \frac{2}{\sqrt{2}}\right) - \frac{3a^3 - 2a^3\sqrt{2}}{6}\pi. \quad (21)$$

Similarly, for a triangular pore, a third of the square of the cluster side can be expressed through the height (22). Then the ratio is reduced to a square equation equated to two-thirds of a side square (23). From here, we obtain a square of the difference between a side and a height, expressed through the square of the cluster's side (24). This indicates the ability to express height through the length of a side (25).

$$\frac{1}{3}a^2 = 2ah - h^2; \quad (22)$$

$$a^2 - 2ah + h^2 = \frac{2}{3}a^2; \quad (23)$$

$$(a - h)^2 = \frac{2}{3}a^2; \quad (24)$$

$$a - \sqrt{\frac{2a^2}{3}} = h. \quad (25)$$

Accordingly, the volume of the fragment cut-off by a particle on a triangular face can also be expressed through the length of a cluster side (26)

$$V_{triang.\,fragm.} = \frac{\pi\left(a - \sqrt{\frac{2a^2}{3}}\right)}{6} \times \left(3\left(\frac{\sqrt{3}}{3}a\right)^2 + \left(a - \sqrt{\frac{2a^2}{3}}\right)^2\right) - \frac{a^3}{96}\pi. \quad (26)$$

Octahedral pores have four faces with the fragments cut off by a triangle, and four hollow faces contact with neighboring pores and do not affect the total volume of a pore. Accordingly, the volume of such octahedron is determined from the standard geometric formula (27)

$$V_{oct} = \frac{1}{3}\sqrt{2}a^3. \quad (27)$$

Accordingly, based on the values of volumes forced out by the particles of pore's fragments (22) and the volume of a virtual octahedron, the volume of an actual octahedral pore (Fig. 5) equals:

$$V_{oct.\,pore} = \frac{1}{3}\sqrt{2}a^3 - 4 \times \left[ \frac{\pi\left(a - \sqrt{\frac{2a^2}{3}}\right)}{6} \left(3\left(\frac{\sqrt{3}}{3}a\right)^2 + \left(a - \sqrt{\frac{2a^2}{3}}\right)^2\right) - \frac{a^3}{96}\pi \right]. \quad (28)$$

Cuboctahedral pores, which are similar to particles, have 6 square faces, cut off by the curvature of particles and 8 triangular faces, which are voids, through which a pore contact with the neighboring ones. The volume of a cuboctahedral polyhedron, which determines the shape of a pore, is determined from the standard geometric formula (29) and is equal to:

$$V_{cubooct} = \frac{5a^3}{3}\sqrt{2}. \quad (29)$$

Accordingly, the volume of an actual cuboctahedral pore (30) will be equal to the difference of volume of a virtual cluster (29) and six volumes, cut-off by a particle on quadrangular faces (21)

$$V_{cubooct.\,pore} = \frac{5a^3}{3}\sqrt{2} - 6 \left[ \frac{\pi\left(a^3 - \frac{a^3}{\sqrt{2}}\right)}{6} \left(3 - \frac{2}{\sqrt{2}}\right) - \frac{3a^3 - 2a^3\sqrt{2}}{6}\pi \right]. \quad (30)$$

Accordingly, the actual volume of a cluster (31), centered around one particle is equal to the sum of volumes of

13 spheres-particles, 8 octahedral pores (28), and 6 cuboctahedral pores (30) due to equality of a side of cluster polyhedrons and radii of particles:

$$V_{cluster} = \frac{52\pi R^3}{3} + \left[ \begin{aligned} &+8 \left( \frac{\frac{1}{3}\sqrt{2}R^3 - \pi \left( R - \sqrt{\frac{2R^2}{3}} \right) \left( 3 \left( \frac{\sqrt{3}}{3} R \right)^2 + \left( R - \sqrt{\frac{2R^2}{3}} \right)^2 \right) - \frac{R^3}{96}\pi}{6} \right) + \\ &+6 \left( \frac{\frac{5R^3}{3}\sqrt{2} - \pi \left( R^3 - \frac{R^3}{\sqrt{2}} \right) \left( 3 - \frac{2}{\sqrt{2}} \right) - \frac{3R^3 - 2R^3\sqrt{2}}{6}\pi}{6} \right) \end{aligned} \right] \cdot \quad (31)$$

HCP packing differs from the FCC packing only by coordinates of the arrangement of contact points and pores. Virtual pores-clusters are represented by a figure that consists of two halves of a cuboctahedron, one of which was rotated by 180 degrees and connected to the other along the axis of symmetry. However, the shape of the pores is determined by the same octahedron and cuboctahedron. The volume of a cluster and the volume of pores remains exactly the same as at FCC packing.

**5. 3. Calculation of load distribution at isostatic pressing based on a model of spongy titanium particles as a spongy body formed by hollow spheres**

The third stage is the formation of stable structures, involving a certain deformation of a particle, which makes it possible to form stable bonds with the neighboring ones, forming a briquette with a large number of internal stresses. This stage is the last one from the early stage of pressing, because in the future the deformation occurs at the macro level in different zones of packing. In particular, it can be observed near the walls of a mold, where the particle deformation without the use of an elastic punch can reach the diametric plane.

When the cluster elements are compressed, the particles in contact points are pressed through. In this way, the geometric packing lattice will look like a truncated cuboctahedron (Fig. 8), circumscribed in a particle. However, the contact between particles, in this case, will occur on quadrangle faces.

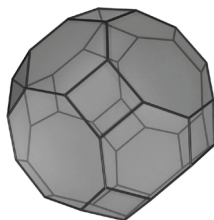


Fig. 8. Cluster at the stage of formation of stable structures

At the non-uniform compression, their dimensions may differ, that is why it is better to calculate each of the axes of symmetry separately.

Accordingly, it is possible to derive the equation of the formation of particle adhesion strength. For this purpose, it is necessary to calculate the areas of contact between particles within the framework of the problem of contact interaction mechanics [20]. Depending on the radius of a particle, pressure in the contact area is distributed according to the equation:

$$p = p_0 \sqrt{1 - \frac{r^2}{a^2}}, \quad (32)$$

where  $p_0$  is the maximum contact pressure that is calculated from formula:

$$p_0 = \frac{3F}{2\pi a} = \frac{\sqrt[3]{6FE^2}}{\pi R^2}, \quad (33)$$

where  $a$  is the radius of the contact plane,

$$a = 0.88 \cdot \sqrt[3]{F \frac{\frac{1}{E_1} + \frac{1}{E_2}}{\frac{1}{R_1} + \frac{1}{R_2}}}, \quad (34)$$

in our case, material and radii of particles are the same, that is why

$$a = 0.88 \cdot \sqrt[3]{F \frac{\frac{2}{E_T}}{\frac{2}{R_1}}}. \quad (35)$$

$K_{update}$  is equaled to the contact plane

$$K_{update} = a = 0.88 \cdot \sqrt[3]{F \frac{\frac{2}{E_T}}{\frac{2}{R_1}}}, \quad (36)$$

then

$$\frac{\sigma_{separation}}{2\tau_s} = \left( 1 - \frac{1}{0.88 \cdot \sqrt[3]{F \frac{\frac{2}{E_T}}{\frac{2}{R_1}}}} \right) \quad (37)$$

The powder composite turns out to be an absolute opposite of metal foam. In metal foam, conditional pore-spheres are represented by direct and inverse cuboctahedrons, and titanium-filled space between them – by octahedrons and cuboctahedrons. At the same time, in powder composite, on the contrary, the pores are represented by octahedrons and cuboctahedrons, and a particle is represented only by a direct or inverse cuboctahedron. The volume of space, concave due to the interaction between two particles, is the sum of volumes destroyed by the pressure of contact interaction of microspheres and calculation volume of an ellipsoid for non-porous titanium

$$V_{cont} = \frac{4}{3}\pi(2a)^2 d, \quad (38)$$

where  $V_{cont}$  is the volume of an ellipsoid of contact for two titanium spheres at the specified loading,  $d = \frac{R}{a^2}$  is the contact depth

The critical stress for microspheres is determined by the criteria of Tresc-Saint-Venan and Huber-Mises [21]:

$$\sigma_{red}^{max} = \frac{2p}{\left(1 - \frac{r_{ext}^2}{r_{int}^2}\right)}, \quad (39)$$

where  $\frac{r_{ext}}{r_{int}}$  is the ratio of the external radius of a sphere to the internal one.

At excess of this magnitude, the microsphere is ruined, which makes it possible to calculate the force applied to destroy the spheres by their average radius.

Pressure in the contact zone is distributed in accordance with the formula for purely titanium spheres, but taking into consideration the force consumed to destroy the microspheres

$$p_{cont} = \frac{\sqrt[3]{6FE^{*2}}}{\pi R^2} \sqrt{1 - \frac{d^2}{a^2} - \frac{\left(1 - \frac{r_{ext}^2}{r_{int}^2}\right)}{2\sigma_{red}^{max}}}, \quad (40)$$

where  $\sigma_{red}^{max}$  is the critical tension of microsphere

Thus, the average radii for microspheres in microns are the following: external  $r_{ext} = 18,1$ , and internal radius  $r_{int} = 17,6$ .

Accordingly, pressure distribution at isostatic pressing is determined by the radius of particles and applied force.

$$p_{cont} = \frac{\sqrt[3]{6FE^{*2}}}{\pi R^2} \sqrt{1 - \frac{R^2}{\left(0,88 \cdot \sqrt[3]{F \frac{E_{Ti}}{2} \frac{2}{R}}\right)^6} - \frac{\left(1 - \frac{r_{ext}^2}{r_{int}^2}\right)}{2 \frac{2F}{0,88 \cdot \sqrt[3]{F \frac{E_{Ti}}{2} \left(1 - \frac{r_{ext}^2}{r_{int}^2}\right)}}}}. \quad (41)$$

Assessing the resulting formula, it is necessary to take into consideration the fact that in the volume of the pressing, the forces spent on the destruction of microspheres can be scarce. At the same time, under the punch, the applied forces are sufficient to deform a particle to the diametric plane.

Based on the above coordinates of the contact zones, it can be noted that the vector of the largest deformation from the interaction of particles propagates in the direction of applying the force. If packing taken as a basis is correct, pressing product is often clearly laminated and density should grow exponentially when approaching the punch.

#### 5.4. Measurement of actual porosity and pressing density, patterns of their dependence on pressing load

When calculating the total thermal conductivity in the general form, one used the Lobb formula (42), based on the conduction of the material, which forms a porous body:

$$\lambda = \lambda_0(1 - \theta), \quad (42)$$

where  $\lambda$  is the conductivity (heat, electric, or in our case, mechanical stresses),  $\lambda_0$  is the initial conductivity,  $\theta$  is the porosity. This approach is not always correct since it does not take into account convection that depends on the condition of using a porous body and thermal radiation, which can be up to 60 % of the total thermal conductivity of the material.

However, it remains important that such a simplified representation of conductivity is displayed in formula (43) to determine the density of porous material:

$$\rho = \rho_k(1 - P), \quad (43)$$

which is similar to the specified one and characterizes density distribution by the volume of a workpiece.

Besides, paper [11] also proposes to apply a similar formula (44) to characterize a change of external friction in a cylindrical mold:

$$\tau_k = f\tau_s(1 - \theta_n), \quad (44)$$

where  $\theta_n$  is the relative surface porosity

$$\theta_n = \frac{S_n}{S}, \quad (45)$$

where  $S_n$  is the relative surface porosity,  $S$  is the contact surface area of porous material,  $\tau_s$  is the boundary of the fluidity of material to a shift in a compact state,  $f$  is the proportionality factor in the Zibbel law of friction.

It is evident that this process is a form of mass transfer, expressed through the transfer of mechanical energy at the deformation of particles. One of the variants of conductivity for pressure.

However, it should be noted that it is inappropriate to rely directly on these models, as in model [9], the clusters were built without taking into consideration the coordination number, so packing of particles into it is rhombic. In real materials, such packing is very unlikely, because spherical particles always tend to fill the space to maximum density. Defects occur when the force of friction between particles creates resistance that is higher than the kinetic energy of a particle. Model [11] describes well the volume properties and filling of intercluster pores at the expense of material fluidity, but does not describe the distribution of forces at the level of a cluster-particle.

To develop a model that will characterize these issues, it is worth considering a series of factors:

1) The near-surface layer directly under the punch and near the edges is deformed to the diametric plane even at a pressure of the order of 1–2 MPa due to pressure and/or force of friction near the walls [13].

2) Particles have their natural porosity, the calculation of which, when applying formula (44), for external friction will enable characterizing the strength of bonds between particles and in a briquette as a whole is most effective.



3) The number of contacts in the clustered model is determined by the coordination number and is equal to 12.

4) There are cluster and intercluster pores in the composite, which are initially open, at an increase in loading are filled through deformation and later the leakage of the material of particles. Such pores can be completely filled, change shape, or become isolated or closed.

The model of density and porosity distribution, depending on the pressing load, should be based on the results of practical measurements. That is why the average volumetric porosity and density of the studied samples were measured. Processing the results of experiments on the CurveExpert software (Fig. 9) demonstrated that the density of the studied samples shows the inverse logarithmic dependence (46), which corresponds to the formula

$$\rho_{comp} = \frac{1}{0.625 - 0.122 \ln(P_{pres})}, \tag{46}$$

where  $\rho_{comp}$  is the density of a composite briquette,  $P_{pres}$  is the pressing pressure

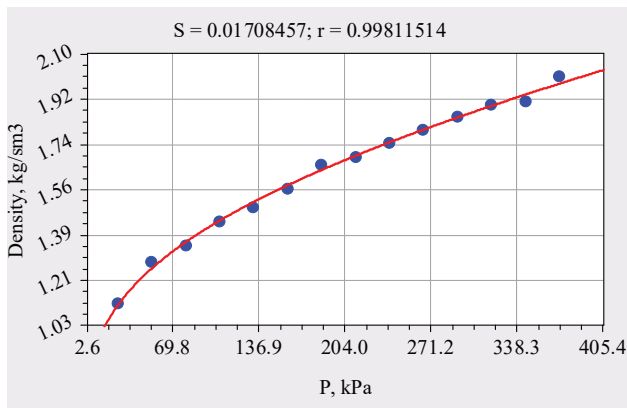


Fig. 9. Dependence of density on pressing pressure

According to experts [18], at pressing powders, the sum of the logarithmic degree of material compaction and logarithmic degree of deformation for three mutually perpendicular directions is zero

$$\ln \frac{h_2}{h_1} + \ln \frac{b_2}{b_1} + \ln \frac{l_2}{l_1} + \ln \frac{\gamma_2}{\gamma_1}, \tag{47}$$

where  $h_1, b_1, l_1$  are the linear dimensions of the volume of compacted material

Taking into consideration that in binary systems with the disordered distribution of components, not conductivities, but rather their logarithms are mixed [22], it is possible to assume that we deal with the conductivity of mechanical energy in heterogeneous material.

And indeed, the vividly pronounced random structure of spongy titanium does not make it possible to predict linearly the transfer of mechanical stresses in the material.

Dependence of porosity on the load (Fig. 10) shows the properties that are opposite to density (at an increase in loading, density increases and porosity falls by exponential dependence (48)

$$P = 0.66 \cdot \exp(-0.15 \cdot P_{pres}). \tag{48}$$

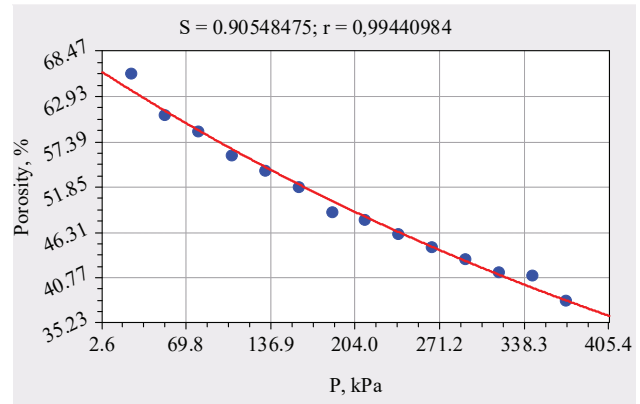


Fig. 10. Dependence of porosity on pressing loading

As it can be seen from the presented data, the logarithmic principle of transfer of mechanical energy in porous bodies is based on the features of packing particles, and the exponential ratio of the porosity to pressing pressure [23] corresponds to the empirical ratio (49):

$$\varepsilon = \varepsilon_0 e^{-\beta P}, \tag{49}$$

where  $\varepsilon_0$  is the porosity at zero pressure (maximum porosity at the compaction stage),  $\beta$  is the compression coefficient.

Accordingly, it makes it possible to identify all the specified values at once, which gives minimal porosity in the absence of pressure from the punch of about 66 %, the compression coefficient for spongy titanium is about 0.15. These indicators are the empirical magnitude, which displays only the average indicator, but this is quite sufficient for calculations.

The developed models are proved by experimental measurements and can be applied to predict the properties of porosity of materials based on spongy titanium.

## 6. Discussion of results of studying the impact of parameters of composite materials on the critical conditions of their usage

The research applies a comprehensive approach, which includes the elements of combinatorics (spheres packing), plastic deformation of metals, mechanics of contact interaction, and organization of binary systems. A substantial improvement of the approach in modeling pore formation processes is its breakdown into stages and classification of pores according to their nature.

Thus, based on the corpuscular spongy classification of the porous bodies [2], it was determined that particles of spongy titanium particles have the shape of a spongy body, and composite material, created using the methods of powder metallurgy – corpuscular. At its core, they are opposites by the character of the arrangement of pores, relative to the material. Based on the coordination number, which in the densest packing is equal to 12, the geometrical cluster model of particle packing in the pressing product was created. Cuboctahedral FCC and HCP packing (Fig. 4) became the basis of this model, which allowed determining a pressed briquette of spongy titanium as a body with corpuscular-spongy porosity.

The resulting model makes it possible to describe clearly the pressing process exactly at the level of a separate particle.

This will allow determining the causes of such problems as vibration vulnerability and thermal crumbling at thermo-scraping the pressed powder briquettes.

This approach will enable avoiding a critical error in the presentation of the distribution of loading on a particle in modeling the structure formation of powder composites [8–11] when the number of contact points does not correspond to the actual one. Though the model of space filling by Kelvin [24], applied by researchers [13] while modeling the load on a given particle, is reasonable, the cluster cuboctahedral model makes it possible to describe the actual processes more accurately.

The basic restriction of this model is the representation of particles packing as similar spheres of the equal form [16–18], which is optimal for the ideal model, but it has drawbacks during applied usage. The model can be used to assess the porosity of composites based on powders with spherical particles.

The main drawback, accordingly, is the impossibility of its use for the mix of powders of different fractions.

Accordingly, a promising way to improve the cluster cuboctahedral model is its development based on Apollonian packing of spheres, taking into consideration the restrictions in diameter of the smallest powder fraction, which should not exceed  $0,256D$  from the largest one.

Calculation of coordinates of contact points of a cluster-particle with neighboring ones will enable approaching directly the creation of high-precision computer models like the Lubachevsky-Stylinger algorithm, but taking into consideration the features of packing.

Since the shape of spongy titanium particles is irregular due to the complex geometry of their surface, the characteristic of the state of the entire pressing product requires either consideration of this particular feature or approximation of the form of particles to the spherical one.

The rolling method of approximation of the shape of particles of spongy titanium to spherical, which is designed as a side result of this study, seems promising. The method will not only enable making the pressing product more predictable but also preserving a part of the natural porosity of particles, turning open pores into closed and isolated. This is especially relevant for materials used as thermal insulation.

The issues of homogenization of particles of spongy titanium were described in papers [12, 13]. However, the reflection of the nature of this particle as a body with a spongy porosity, formed by Apollonian packing of hollow titanium pores-microspheres, is not considered in similar studies.

It is taking into consideration the key difference between the deformation of two elastic spheres and deformation of the conglomerate of microspheres with their critical destruction by the criteria of Tresca-Saint-Venant and Huber-Mises [21] that will enable accurate characterization of displacement of a cluster face and strength of particles' soldering by pressure.

The main drawback of this calculation is the complexity of predicting the arrangement of microspheres in a particle, which in this study required the use of average indicators.

The solution to this problem requires additional simulation of the spongy pore formation processes during magnesium reduction of titanium, which is currently conducted. It is also necessary to take into consideration the principles of formation of particles' surface, including the destruction of microspheres due to displacement and interaction with sharp edges of destroyed microspheres of another particle.

The study of the dependence of density and porosity of pressed spongy titanium briquettes on the load at isostatic

pressing enables characterizing the properties of pressing products at all-sided compression.

Relying on the statement [22] that not conductivities, but their logarithms are mixed in binary systems with the disordered distribution of components, the formation of density can be characterized as the conductivity of mechanical energy in the heterogeneous medium.

The study of pressed samples of spongy titanium briquettes demonstrated such dependence of porosity of loading, which allows relying on the empirical ratio (49), by the author of [23]. This gives a compression coefficient for spongy titanium of around 0.15 and porosity at the compaction stage of about 66 %.

In the long term, the cluster model of packing of particles and the results of applied research, improved due to consideration of segregation and spatial stratification of particles, will enable developing an additive technology for the layered formation of corpuscular-spongy composites based on spongy titanium.

The applied aspect of using the obtained scientific result is the possibility of reducing the typical technological process for obtaining pressing products of spongy titanium to the form of one of the variations of additive technologies with assigning the structure at the level of position of each particle. This makes the preconditions to transfer the received technological solutions to foundry production and to obtain composite materials for military-civilian purposes.

---

## 7. Conclusions

---

1. Models of formation of each type of pores and their arrangement in a mold in relation to cluster particles were developed. It was proposed to use cuboctahedrons as clusters because their number of faces corresponds to coordination number and makes it possible to estimate the shape of pores and the method of particle packing. The packing density, which corresponds to the FCC and HCP packing of spheres with coordination number 12, is maximum without deformation. Three kinds of pores were separated in the developed clustered model: clustered, having a cuboctahedral shape; intercluster with the shape of a cuboctahedron and octahedron; natural pores of a material having a shape of microspheres.

2. The coordinates of contact points of particles with the neighboring particles relative to the geometric center of a cluster, which under real conditions will be in the particle mass center, were presented. The difference between the FCC and HCP packing only at 3 points was determined. Since actual pores are concave Steiner cuboctahedrons and octahedrons, the difference between the geometric and physical model of a pore is expressed in the subtraction of volume of ellipsoid quarters in the appropriate areas.

3. It was determined that spongy titanium is a totality of hollow spheres – a typical metal sponge with spongy porosity. The powder pressed composite is its direct opposite with corpuscular porosity. The formula of pressure distribution at isostatic pressing was created, based on taking into consideration the destruction of spheres as a deformation factor in elastic interaction of two spheres.

4. Actual measurements show the average exponential ratio of the porosity to pressing pressure, which makes it possible to calculate maximum intercluster porosity at boundary compaction of 66 % and compression factor of tested material of 0.15.

## References

1. Krivoruchko, Y. S., Lerman, L. B., Shkoda, N. G. (2013). Models of porous medias. *Poverhnost'*, 5, 34–47. Available at: [http://nbuv.gov.ua/UJRN/Pov\\_2013\\_5\\_6](http://nbuv.gov.ua/UJRN/Pov_2013_5_6)
2. Kiselev, A. V. (1958). *Korpuskulyarnaya struktura adsorbentov geley. Metody issledovaniya struktury vysokodispersnyh i poristyh tel.* Moscow, 47–59.
3. Pałka, K., Pokrowiecki, R. (2018). Porous Titanium Implants: A Review. *Advanced Engineering Materials*, 20 (5), 1700648. doi: <https://doi.org/10.1002/adem.201700648>
4. Naidich, Y. V., Krasovskii, V. P. (2015). Use of Interfacial Exothermic Effect in the Wetting Process, Production of Composites, and Soldering of Ceramic Materials. *Powder Metallurgy and Metal Ceramics*, 54 (5-6), 331–339. doi: <https://doi.org/10.1007/s11106-015-9718-3>
5. Zabolotnyi, O., Sychuk, V., Somov, D. (2018). Obtaining of Porous Powder Materials by Radial Pressing Method. *Advances in Design, Simulation and Manufacturing*, 186–198. doi: [https://doi.org/10.1007/978-3-319-93587-4\\_20](https://doi.org/10.1007/978-3-319-93587-4_20)
6. Romero, C., Yang, F., Bolzoni, L. (2018). Fatigue and fracture properties of Ti alloys from powder-based processes – A review. *International Journal of Fatigue*, 117, 407–419. doi: <https://doi.org/10.1016/j.ijfatigue.2018.08.029>
7. Hadadzadeh, A., Whitney, M. A., Wells, M. A., Corbin, S. F. (2017). Analysis of compressibility behavior and development of a plastic yield model for uniaxial die compaction of sponge titanium powder. *Journal of Materials Processing Technology*, 243, 92–99. doi: <https://doi.org/10.1016/j.jmatprotec.2016.12.004>
8. Titov, V. G., Zalazinskii, A. G., Kryuchkov, D. I., Nesterenko, A. V. (2019). Multi-criteria optimization by the «ideal point» method of raw material composition for composite blank manufacturing. *Izvestiya Vuzov. Poroshkovaya Metallurgiya i Funktsional'nye Pokrytiya (Universities' Proceedings. Powder Metallurgy And Functional Coatings)*, 2, 49–56. doi: <https://doi.org/10.17073/1997-308x-2019-2-49-56>
9. Berezin, I. M., Zalazinskii, A. G., Nesterenko, A. V., Bykova, T. M. (2019). Simulation of metal powder bidirectional compression in a pressing tool with a floating die. *PNRPU Mechanics Bulletin*, 3, 5–16. doi: <https://doi.org/10.15593/perm.mech/2019.3.01>
10. Berezin, I., Nesterenko, A., Kovacs, G., Zalazinskii, A. (2017). Influence of Stress State Conditions on Densification Behavior of Titanium Sponge. *Acta Polytechnica Hungarica*, 14 (6), 153–168.
11. Zalazinskii, A. G., Nesterenko, A. V., Berezin, I. M. (2019). Study of the process of titanium-containing furnace charging material compaction by an experimental-analytical method. *Izvestiya Vuzov Tsvetnaya Metallurgiya (Proceedings of Higher Schools Nonferrous Metallurgy)*, 4, 16–22. doi: <https://doi.org/10.17073/0021-3438-2019-4-16-22>
12. Savich, V. V., Taraykovich, A. M., Sheko, G. A., Bedenko, S. A. (2017). Increase in homogenization of bidisperse mixture of spongy titanium powders and reduction in energy consumption during its preparation in the production of thin permeable elements. *Metal Powder Report*, 72 (5), 327–330. doi: <https://doi.org/10.1016/j.mprp.2016.04.006>
13. Savich, V. V., Pronkevich, S. A., Sheluhina, A. I., Gorohov, V. M. (2013). Modelirovanie deformatsii chastitsy nesfericheskogo poroshka titana pri odностороннем прессовании пуансоном, plakirovany elastichnoy oblitsovkoy. *Poroshkovaya metallurgiya: Inzheneriya poverhnosti, novye poroshkovye kompozitnye materialy, svarka. Sbornik dokladov 8-go Mezhdunarodnogo simpoziuma.* Minsk, 314–320.
14. Klymenko, L. P., Andrieiev, V. I., Prishchepov, O. F., Shuhai, V. V., Sluchak, O. I. (2017). Modification of construction and composite mixture in casting forms for cylinders of ICE. *Internal Combustion Engines*, 1, 43–46. doi: <https://doi.org/10.20998/0419-8719.2017.1.08>
15. Andreeva, N. V., Radomysel'skiy, I. D., Scherban', N. I. (1975). *Issledovanie uplotnyaemosti poroshkov.* *Poroshkovaya metallurgiya*, 6, 32–42.
16. Ferguson, S. P., Hales, T. C. (1998). A formulation of the Kepler conjecture. arXiv. Available at: <https://arxiv.org/pdf/math/9811072.pdf>
17. Konvey, Dzh., Sloen, N. (1990). *Upakovki sharov, reshetki i gruppy.* Moscow: Mir, 415.
18. Conway, J. H., Sloane, N. J. A. (1998). *Sphere Packings, Lattices and Groups.* Springer. doi: <https://doi.org/10.1007/978-1-4757-2016-7>
19. Donets', A. G. (2000). Pro vzazheni zadachu Shteynera. *Matematychni mashyny i systemy*, 1, 28–37.
20. Johnson, K. L. (1985). *Contact Mechanics.* Cambridge University Press. doi: <https://doi.org/10.1017/cbo9781139171731>
21. Batyanovskiy, E. I., Leonovich, I. A., Leonovich, A. A. (2010). Rezhimy pressovaniya materialov, porizovannyh mikrosferami. *Novye materialy i tekhnologii v mashinostroenii: materialy XII Mezhdunar. nauch. Internetkonf. Bryansk: BGITA*, 12, 151–155.
22. Lichtenecker, K. (1926). Die Dielektrizitatskonstante naturlicher und Kunstlicher Mischkorper. *Physik Z*, 27, 115–255.
23. Shneyder, P. (1960). *Inzhenernye problemy teploprovodnosti.* Moscow: Izdatel'stvo inostrannoy literatury, 478.
24. Thomson, W. (1887). LXIII. On the division of space with minimum partitional area. *The London, Edinburgh, and Dublin Philosophical Magazine and Journal of Science*, 24 (151), 503–514. doi: <https://doi.org/10.1080/14786448708628135>